

Which Interactions Dominate in Active Colloids?

Benno Liebchen^{1,*} and Hartmut Löwen¹

¹*Institut für Theoretische Physik II: Weiche Materie,
Heinrich-Heine-Universität Düsseldorf, D-40225 Düsseldorf, Germany*

(Dated: April 18, 2022)

Active colloids, which self-propel by producing a chemical gradient across their own surface, serve as versatile microengines sparking a huge potential for the creation of functional materials through nonequilibrium self-assembly. Despite a mounting evidence that the same gradients which are used for swimming induce important cross-interactions among active colloids (phoretic interaction), they are still ignored in most many-body descriptions, perhaps to avoid complexity and a zoo of unknown parameters. Here we derive a simple model for active colloids, which shows that phoretic interactions are the dominant interaction in canonical active colloids (rather than hydrodynamic interactions) and are controlled by one genuine parameter - the self-propulsion speed. Unlike present standard models, but in accordance to canonical experiments, the model predicts dynamic clustering as a generic outcome. The present work massively simplifies descriptions of active colloids including their key interactions and allows to directly include phoretic interactions in Brownian dynamics simulations and generic field theories.

Introduction Active colloids [1, 2], first realized at the turn to the 21st century [3, 4], have experienced a steep evolution: now, they serve as a platform for the creation of functional devices and are used, for example, as microengines [1, 5–7] and cargo-carriers [8, 9] aimed to deliver drugs towards cancer cells in the future. These colloids self-propel by catalyzing a chemical reaction on part of their surface, creating a gradient which couples to the surrounding solvent and drives the colloids forward. When many active colloids come together, they self-organize into spectacular patterns, which would be impossible in equilibrium, but offer huge perspectives for the creation of new materials through nonequilibrium self-assembly [10–17]. A typical pattern, reoccurring in canonical experiments with active Janus colloids, are so-called living clusters which spontaneously emerge at remarkably low densities (area fraction 3 – 10%) and dynamically split up and reform as time proceeds [10, 18–20]. When trying to understand such collective behaviour in active colloids, we are facing complex setups of motile particles showing multiple competing interactions, such as steric, hydrodynamic and phoretic ones (the latter ones hinge on the cross-action of self-produced chemicals on other colloids).

Therefore, to reduce complexity and allow for descriptions which are simple enough to promote our understanding of the colloids' collective behaviour, yet sufficiently realistic to represent typical experimental observations (such as dynamic clustering) we have to resolve the quest: which interactions dominate in active colloids? - the topic of the present letter. Presently, the most commonly considered models in the field, like the popular Active Brownian particle model [21, 22] and models involving hydrodynamic interactions [23, 24] neglect phoretic interactions altogether, perhaps to avoid complexity and

the set of unknown parameters their description usually brings along. Conversely, recent experiments [10, 14, 18] and theories [25] suggest a crucial importance of phoretic interactions in active colloids - which leaves us with a conflict calling for clarification.

Here, we show that phoretic interactions generically dominate over hydrodynamic interactions in typical active colloids. As opposed to (biological) microswimmers moving by body-shape deformations [23, 26–34], hydrodynamic interactions can therefore be neglected in the description of active colloids, but not phoretic interactions. As our key result, we systematically derive a new model, the Active Attractive Alignment model (AAA model), providing a strongly reduced but essentially realistic description of typical active colloids. In particular, the AAA model reduces phoretic interactions to a simple pair interaction among the colloids whose strength is controlled by one genuine parameter, the self-propulsion speed (or Peclet number). This allows to include them e.g. in Brownian dynamics simulations, rather than requiring hybrid particle-field descriptions and releases their modeling from the zoo of unknown parameters it usually involves [35–38]. As its generic behaviour at low density and as opposed to present standard models of active colloids, the AAA model predicts dynamic clustering at low density, in agreement with experiments [10, 18–20]. The present work focuses on attractive phoretic interactions as probably relevant to most experiments and is complementary to [25] which mainly focuses on cases where phoretic interactions are repulsive and can be dominated by delay effects. Our work should be useful e.g. to model active colloids and to design active self-assembly [14, 39, 40].

Phoretic motion in external gradients: When exposed to a gradient in an externally imposed phoretic field c , which may represent e.g. a chemical concentration field, the temperature field or an electric potential, colloids move due to phoresis. Here, the gradients in c act on the fluid elements in the interfacial layer of the colloid

* liebchen@hhu.de

and drive a localized solvent flow tangentially to the colloidal surface with a velocity, called slip velocity

$$\mathbf{v}_s(\mathbf{r}_s) = \mu(\mathbf{r}_s)\nabla_{\parallel}c(\mathbf{r}_s) \quad (1)$$

Here \mathbf{r}_s is a point immediately above the colloidal surface and $\nabla_{\parallel}c$ is the projection of the gradient of c onto the tangential plane of the colloid. The colloid moves opposite to the average surface slip with a velocity [41] $\mathbf{v} = \langle -\mathbf{v}(\mathbf{r}_s) \rangle$ where brackets represent the average over the colloidal surface. If the solvent slips asymmetrically over the colloidal surface, the colloid also rotates with a frequency [41] $\Omega = \frac{3}{2R}\langle \mathbf{v}(\mathbf{r}_s) \times \mathbf{n} \rangle$ where R, \mathbf{n} are the radius and the local surface normal of the colloid. Performing surface integrals, specifically for a Janus colloid with a catalytic hemisphere with uniform surface mobility μ_C and a mobility of μ_N on the neutral side, yields:

$$\mathbf{v}(\mathbf{r}) = -\frac{\mu_C + \mu_N}{3}\nabla c; \quad \Omega(\mathbf{r}) = \frac{3(\mu_C - \mu_N)}{8R}\mathbf{e} \times \nabla c \quad (2)$$

Here, we evaluate c at the colloid center \mathbf{r} for simplicity, and have introduced the unit vector \mathbf{e} pointing from the neutral side to the catalytic cap.

Self-propulsion Autophoretic colloidal microswimmers, or active colloids, self-produce phoretic fields on part of their surface with a local surface production rate $\sigma(\mathbf{r}_s)$. In steady state, we can calculate the self-produced field by solving the chemical diffusion equation

$$0 = D_c \nabla^2 c + \oint d\mathbf{x}_i \delta(\mathbf{r} - \mathbf{r}_i(t) - R\mathbf{x}_i) \sigma(\mathbf{x}_i) - k_d c \quad (3)$$

where the sink term $-k_d c$ represents an effective decay of the relevant phoretic field (chemicals, heat, ions), which may result e.g. from secondary chemical reactions taking place in the solvent, or heat absorption processes. While so-far neglected in most of the literature, Fig. 1 shows that such a sink term should be included when describing phoretic interactions among active colloids as we shall see below. Conversely, self-propulsion, i.e. the phoretic drift of a colloid in its self-produced gradient, depends only on the phoretic field close to the colloid surface, so that we can ignore the decay. Considering Janus colloids which produce chemicals with a local rate $\sigma = k_0/(2\pi R^2)$ on one hemisphere and $\sigma = 0$ on the other one, solving Eq. (3) for $k_d = 0$ and using (1.), we find its self-propulsion velocity [6]

$$\mathbf{v}_0 = -\frac{k_0(\mu_N + \mu_C)}{16\pi R^2 D_c} \mathbf{p} \quad (4)$$

For symmetry reasons the considered Janus colloids do not show self-rotations.

How strong are phoretic interactions? Besides leading to self-propulsion, the gradients produced by an autophoretic colloid also act in the interfacial layer of all other colloids. Here, they drive a solvent slip over the colloids' surfaces, which induce a phoretic translation and a rotation. Following Eqs. (1,2,4) a colloid at the origin

causes a translation and rotation of a test Janus colloid at position \mathbf{r} with

$$\mathbf{v}_P(\mathbf{r}) = -\nu \frac{16\pi R^2 D_c v_0}{3k_0} \nabla c; \quad \Omega_P(\mathbf{r}) = \mu_r \nu \frac{6D_c \pi R v_0}{k_0} \nabla c \quad (5)$$

Here, $\nu = -1$ for swimmers moving with their catalytic cap ahead and $\nu = 1$ for cap-behind swimmers [25]; we have further used $v_0 = |\mathbf{v}_0|$ and have introduced the reduced surface mobility $\mu_r = (\mu_C - \mu_N)/(\mu_C + \mu_N)$. Now solving Eq. (3) in far-field, yields the chemical field produced by the colloid at the origin

$$c(\mathbf{r}) = \left[\frac{k_0}{4\pi D_c r} \mp \frac{R}{4(2\pi)^{5/2}} \frac{\hat{\mathbf{p}} \cdot \hat{\mathbf{r}}}{r^2} + \mathcal{O}\left(\frac{1}{r^3}\right) \right] e^{-\kappa r} \quad (6)$$

where $\kappa = \sqrt{k_d/D_c}$ is an effective inverse screening length; the case $\kappa = 0$ corresponds to absence of screening. Finally combining Eqs. (3) and (5) yields, in leading order

$$\begin{aligned} \mathbf{v}_P(\mathbf{r}) &= \frac{-4v_0 R^2 \nu}{3} \nabla \frac{e^{-\kappa r}}{r} \\ \Omega_P(\mathbf{r}) &= \frac{-3v_0 R \mu_r}{2} \mathbf{p} \times \nabla \frac{e^{-\kappa r}}{r} \end{aligned} \quad (7)$$

where \mathbf{p} is the unit vector pointing from \mathbf{r} into the swimming direction of the test colloid.

Modulo factors of order 1 and κ , the prefactors in Eqs. (7) only depend on the self-propulsion velocity and the colloidal radius, which are well known in experiments. We now exploit this explicit knowledge of the strength of phoretic interactions for a comparison with hydrodynamic interactions. In bulk, the hydrodynamic flow field of a phoretically moving colloid (well beyond its interfacial layer) reads, at a point \mathbf{r} relative to its center [42]

$$\mathbf{v}(\mathbf{r}) = \frac{1}{2} \left(\frac{R}{r} \right)^3 (3\hat{\mathbf{r}}\hat{\mathbf{r}} - I) \cdot \mathbf{v}_0 \quad (8)$$

This velocity advects other colloids and can be compared with the translation velocity induced by phoretic interactions. For a rough estimate of the relative strength of phoretic and hydrodynamic interactions (in far field) we use (7, left) and (8) to define a parameter $m(r) = 8r^3/(3R)|\partial_r(\exp[-\kappa r]/r)|$. When $m > 1$ phoretic interactions should dominate, whereas $m < 1$ means that hydrodynamic interactions are stronger. Without chemical decay ($\kappa = 0$) as assumed in most parts of the literature [10, 14, 35–37] we have $m \gg 1$ at all relevant distances (i.e. all but very short distances where near field effects take over anyway), i.e. phoretic interactions generally dominate. For $\kappa > 0$, hydrodynamic interactions might dominate at long distances, but not at typical ones. For a typical suspension of colloids with $R = 1\mu\text{m}$ at 10% area fraction (average distance $5.6\mu\text{m}$) and a screening length of $\kappa R = 0.25$ (Fig. 1), we find $m \sim 9$, and even for $\kappa R \sim 0.5$, we have $m \sim 4$; at higher densities, the dominance of phoretic interactions should be even more

pronounced. In addition to this, the translational component of the phoretic interactions (i.e. \mathbf{v}_P) are isotropic, which may further support them as compared to hydrodynamic interactions which are constrained by the incompressibility condition. Clearly, the present estimates apply to cases of low or moderate density; at high density hydrodynamic near field interactions might become more relevant [43, 44].

We can further see from Eqs. (8) that colloids at a typical distances of $\sim 5R$, approach each other (for $\nu = 1$) within a few seconds (this is consistent with experiments, e.g. [10, 14]); at shorter distances the phoretic translation speed becomes comparable to the self propulsion speed, i.e. $\mathbf{v}_P \sim v_0$. A typical rotation rates, for colloids with $R = 1\mu m$, $v_0 \sim 10\mu m/s$, is $|\boldsymbol{\Omega}| \sim 0.4/s$, i.e. colloids may approach each other before they manage to fully turn (align) their self-propulsion direction. Thus, it is plausible that when forming clusters, they do not show much orientational order [20].

The Active Attractive Aligning Model We now use the above results to construct a model for the collective behaviour of N active particles based on a formal mapping (or identification) of phoretic translations and rotations to forces and torques. As a starting point, let's consider the Active Brownian particle model. Using $t_u = 1/D_r$ where D_r is the translational diffusion rate and $x_u = R$ as time and space units and the Peclet number $Pe = v_0/(D_r R)$ measuring the run length in units of the particle radius, in its most commonly used form this model reads (in dimensionless units)

$$\dot{\mathbf{x}}_i = Pe \mathbf{p}_i + \mathbf{f}_s(\mathbf{x}_i); \quad \dot{\theta}_i = \sqrt{2}\eta_i(t) \quad (9)$$

and describes particles which sterically repel each other (here represented by dimensionless forces \mathbf{f}_s preventing particles to overlap at short distances) and self-propel with a velocity v_0 in directions $\mathbf{p}_i = (\cos \theta_i, \sin \theta_i)$ ($i = 1..N$) which change due to rotational Brownian diffusion; here η_i represents Gaussian white noise with zero mean and unit variance. As its key phenomenon, this model leads to motility-induced phase separation spontaneously emerging from the uniform phase at area fractions of about 30 – 40 per cent if the Peclet number is sufficiently large [19, 22, 45–50]; the typical observation in simulations of this model are clusters which coarsen at late times proceeding towards complete phase separation. Following Eq. (7) and exploiting linearity of Eq. (6), we can now account for phoretic interactions leading to the “Active Attractive Aligning Model”, or AAA model, which we define in quasi-2D as:

$$\begin{aligned} \dot{\mathbf{x}}_i &= Pe \mathbf{p}_i - \frac{4Pe\nu}{3} \nabla u + \mathbf{f}_s(\mathbf{x}_i) \\ \dot{\theta}_i &= \frac{-3Pe\mu_r}{2} \mathbf{p}_i \times \nabla u + \sqrt{2}\eta_i(t) \end{aligned} \quad (10)$$

Here, $\nabla u = \sum_{j=1}^N \nabla_{\mathbf{x}_i} \frac{e^{-\alpha x_{ij}}}{x_{ij}}$ with $x_{ij} = |\mathbf{x}_i - \mathbf{x}_j|$ and $\mathbf{a} \times \mathbf{b} = a_1 b_2 - a_2 b_1$ for 2D vectors \mathbf{a}, \mathbf{b} and where we have

introduced a screening number $\alpha = R\sqrt{k_d/D_c}$. In our simple derivation, we have mapped (or identified) force free translations and rotations as induced by phoretic interactions with formally identical expressions representing reciprocal interaction forces and (nonreciprocal) torques. The resulting expressions represent isotropic Yukawa interaction (Coulomb for $\alpha = 0$) among the colloids and an alignment component (taxis) acting on the self-propulsion direction of the colloids. Remarkably, for a given screening number (typical values might be $\alpha \lesssim 0.3 - 0.6$, Fig. 1), the strength of the phoretic interactions is largely determined by one genuine parameter - the Peclet number - constituting a collapse of parameter space. The coefficients μ_r, ν determine the sign of the interactions: swimmers which self-propel with their cap-ahead ($\nu = -1$) move towards other colloids (attractive phoretic interactions); and those swimming with their cap behind, move away from other colloids (repulsive phoretic interactions). If $\mu_r < 0$ (for thermophoretic swimmers [51, 52] we have $\mu_r \approx -1$) particles turn their self-propulsion direction away from regions of high particle density (negative taxis); if $\mu_r > 0$ which might be the relevant case for diffusiophoretic swimmers, particles on average swim towards regions of high particle density.

Properties of the AAA model (i) The AAA model can be implemented in Brownian dynamics simulations, no longer requiring hybrid descriptions of particles coupled to self-produced fields. (ii) When neglecting the alignment interactions; the AAA model reduces to active Brownian particles with attractions [48, 53–55]; however, as opposed to these phenomenological models, the interaction strength is essentially fixed by the Peclet number here. (iii) Universality: The AAA model applies independently of the type of phoretic mechanism underlying the colloids' self-propulsion (diffusiophoresis, thermophoresis etc.). However, conversely e.g. to pure thermophoretic swimmers, diffusiophoretic swimmers respond both to gradients in the fuel and produce species. Due to linearity of the equations involved in its derivation, the AAA model still applies to such cases if both species are similarly screened. (iv) Delay effects: When the colloids respond with a significant delay to their self-produced fields, which can happen even for very large D_c [25], the AAA model becomes invalid in corresponding parameter regimes; presumably this is relevant mainly for repulsive phoretic interactions [25]. (v) Reciprocity, mixtures and self-assembly: The Yukawa attractions/repulsions in Eqs. (10) are reciprocal only when considering identical colloids. For mixtures of nonidentical Janus colloids, active-passive mixtures or heterogeneous mixtures of uniformly coated colloids the Yukawa interactions in Eqs. (10) become nonreciprocal and induce a net motion [16, 39, 56]. For example, passive particles can be included in the AAA model via the equation of motion $\dot{\mathbf{r}}_i = -(4/3)\mu\nu Pe \nabla_{\mathbf{x}_i} u(\mathbf{x}_i)$ where Pe is the Peclet number of the active colloids and $\mu = 2\mu_P/(\mu_N + \mu_C)$ with μ_P being the surface mobility of the (isotropic) passive colloid. (vi) For single-specied isotropically coated col-

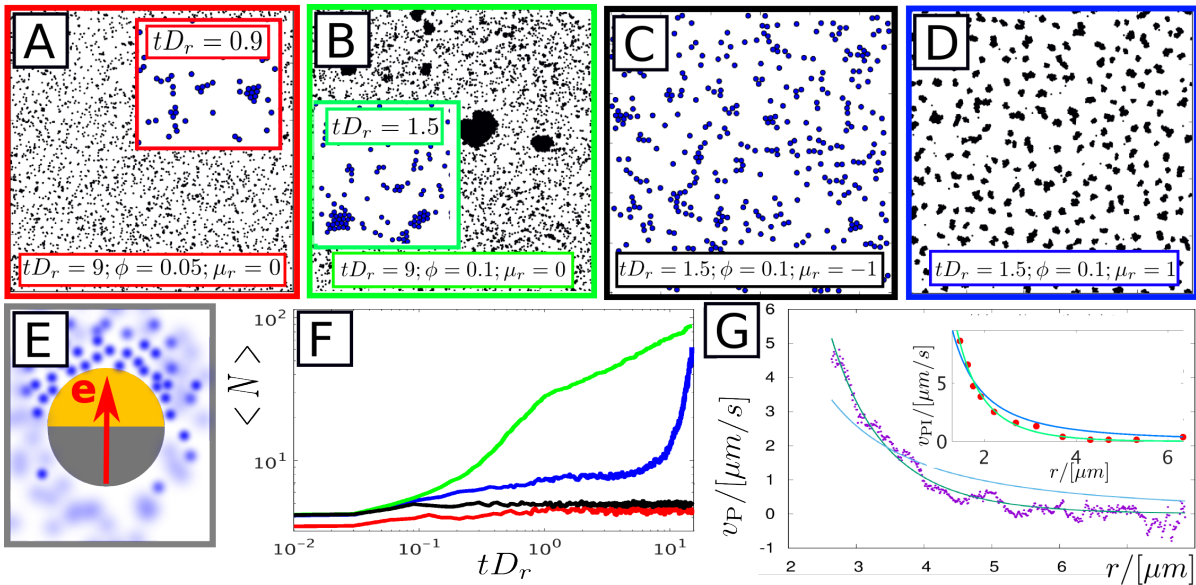


FIG. 1. A-D: Dynamic Clustering in the AAA model; snapshots from Brownian dynamics simulations for 400 – 8000 particles with $\text{Pe} = 100$, $\alpha = 0.25$ at area fractions and times given in the key. Panels A-C show dynamic clusters which continuously emerge and split up; at late times, we observe a finite (nonmacroscopic) cluster size in A,C, but not in B where clusters proceed growing; D shows a ‘chemotactic collapse’. E: Schematic of a Janus colloid swimming with its catalytic cap ahead ($\eta = 1$). F: Time-evolution of the mean cluster size calculated by putting a grid with spacing $2x_u$ over the simulation box and counting connected regions; colors refer to frame colors in A-D G: Velocity of passive tracers due to the phoretic field produced by Janus colloids in experiments [14] (main figure, dots show our own averages over tracer trajectories) and [10] (inset; dots are based on Fig. 2B in [10]). Green and blue curves show fits with and without effective screening respectively. The fits provide us with an (upper) estimate for the screening number $\alpha \lesssim (0.25 - 0.65)$ in both cases; they can be also used to estimate μ for active-passive mixtures, yielding $\mu = 2\mu_P/(\mu_N + \mu_C) \sim 2 - 3$ for [10] and $\mu \gtrsim 5$ for [14].

loids the self-propulsion term vanishes in Eqs. (10) and the AAA model reduces to the hard-core Yukawa model (when accounting for translational diffusion). This shows that chemically active colloids can be used to realize the hard-core Yukawa model (both with attractive or repulsive interactions), which has been widely used to describe effective interactions between charged colloids [57, 58], globular proteins [59] and fullerenes [60]. (vii) Generalizations of the AAA model to 3D are straightforward; here we have $\mathbf{p}_i = -(3/2)\text{Pe}\mu_r(I - \mathbf{p}_i\mathbf{p}_i)\nabla u + \sqrt{2}\boldsymbol{\eta}_i \times \mathbf{p}_i$ where \mathbf{p}_i is the 3D unit vector representing the swimming direction of particle i and $\boldsymbol{\eta}_i$ represents Gaussian white noise of zero mean and unit variance.

Dynamic Clustering in the AAA Model The AAA model generically leads to dynamic clustering at low densities. We show this using Brownian dynamics simulations (Fig. 1). For attractive phoretic interactions at $\text{Pe} = 100$ and $\alpha = 0.25$, we observe the following: (i) Without alignment ($\mu_r = 0$) clusters dynamically emerge, break up and move through space, like in the canonical experiments with active colloids [10, 18–20]. For an area fraction of $\phi = 5\%$, these clusters do not grow beyond a certain size (red line in Fig. 1 F); conversely, for $\phi = 10\%$ once a cluster has reached a certain size (Fig. 1 B), it does not break any further and grows (panel E, green line). The cluster size distribution (not shown) is approximately algebraic at small sizes and de-

cays exponentially at larger sizes, also as in experiments [20]. (ii) Similarly, for $\mu_r = -1$ (negative taxis), we also find dynamic clusters (panel C), here negative taxis stabilizes the dynamic cluster phase and clusters do not grow at late times, even for $\phi = 0.1$ (black curve in F) and for $\phi = 0.2$ (not shown). This combination of attractive translation combined with negative taxis resembles [36]. (iii) For $\mu_r = 1$ where particles turn their swimming direction towards each other (positive taxis), alignment supports aggregation and clusters do not break up; instead particles form rigid clusters from which they rarely escape (panel D); these clusters grow through coalescence at late times.

Note that the clusters seen in (i),(ii) differ from those occurring as a precursor of motility-induced phase separation in the (repulsive) Active Brownian particle (ABP) model [19, 22, 45–50]. More specifically, the ABP model only leads to very small and short lived clusters at typical area fractions of 3–10%; here the cluster size distribution decays exponentially with the number of particles in the cluster (unless we are at area fractions of $\gtrsim 30\%$, close to the transition to motility induced phase separation). In contrast, both in experiments and in the AAA model, we see significant clusters at low area fractions, with a cluster size distribution decaying rather algebraically with size [10, 18–20].

Conclusions The answer to the title question is that phoretic interactions dominate in typical autophoretic colloids whereas hydrodynamic interactions can be approximately neglected at low and moderate density. Our key result, the AAA model, allows to directly include phoretic interactions in Brownian dynamics simulations and in standard field theories of active matter and shows that their strength is controlled by one genuine param-

eter, the swimming speed (Peclet number), rather than involving multiple unknown parameters as in most previous descriptions. The AAA model offers the to-date simplest microscopic model of active colloids agreeing with canonical experiments showing dynamic clustering and should be useful e.g. to design active self-assembly.

Acknowledgements We thank Frederik Hauke for making Fig. 1G (main panel) available.

-
- [1] C. Bechinger, R. Di Leonardo, H. Löwen, C. Reichhardt, G. Volpe, and G. Volpe, *Rev. Mod. Phys.* **88**, 045006 (2016).
- [2] J. L. Moran and J. D. Posner, *Ann. Rev. Fluid Mech.* **49**, 511 (2017).
- [3] W. F. Paxton, K. C. Kistler, C. C. Olmeda, A. Sen, S. K. St. Angelo, Y. Cao, T. E. Mallouk, P. E. Lammert, and V. H. Crespi, *J. Am. Chem. Soc.* **126**, 13424 (2004).
- [4] J. R. Howse, R. A. L. Jones, A. J. Ryan, T. Gough, R. Vafabakhsh, and R. Golestanian, *Phys. Rev. Lett.* **99**, 048102 (2007).
- [5] T. R. Kline, W. F. Paxton, T. E. Mallouk, and A. Sen, *Angew. Chem. Int. Ed.* **44**, 744 (2005).
- [6] R. Golestanian, T. B. Liverpool, and A. Ajdari, *New J. Phys.* **9**, 126 (2007).
- [7] S. J. Ebbens and D. A. Gregory, *Acc. Chem. Res.* (2018).
- [8] X. Ma, K. Hahn, and S. Sanchez, *J. Am. Chem. Soc.* **137**, 4976 (2015).
- [9] A. F. Demirörs, M. T. Akan, E. Poloni, and A. R. Studart, *Soft Matter* **14**, 4741 (2018).
- [10] J. Palacci, S. Sacanna, A. P. Steinberg, D. J. Pine, and P. M. Chaikin, *Science* **339**, 936 (2013).
- [11] S. H. Klapp, *Curr. Opin. Colloid Interface Sci.* **21**, 76 (2016).
- [12] C. Maggi, J. Simmchen, F. Saglimbeni, J. Katuri, M. Dipalo, F. De Angelis, S. Sanchez, and R. Di Leonardo, *Small* **12**, 446 (2016).
- [13] J. Zhang, J. Yan, and S. Granick, *Angew. Chem. Int. Ed.* **55**, 5166 (2016).
- [14] D. P. Singh, U. Choudhury, P. Fischer, and A. G. Mark, *Adv. Mater.* **29** (2017).
- [15] H. R. Vutukuri, B. Bet, R. Roij, M. Dijkstra, and W. T. Huck, *Sci. Rep.* **7**, 16758 (2017).
- [16] F. Schmidt, B. Liebchen, H. Löwen, and G. Volpe, *arXiv preprint arXiv:1801.06868* (2018).
- [17] A. Aubret, M. Youssef, S. Sacanna, and J. Palacci, *Nat. Phys.* (2018).
- [18] I. Theurkauff, C. Cottin-Bizonne, J. Palacci, C. Ybert, and L. Bocquet, *Phys. Rev. Lett.* **108**, 268303 (2012).
- [19] I. Buttinoni, J. Bialké, F. Kümmel, H. Löwen, C. Bechinger, and T. Speck, *Phys. Rev. Lett.* **110**, 238301 (2013).
- [20] F. Ginot, I. Theurkauff, F. Detcheverry, C. Ybert, and C. Cottin-Bizonne, *Nat. Comm.* **9**, 696 (2018).
- [21] P. Romanczuk, M. Bär, W. Ebeling, B. Lindner, and L. Schimansky-Geier, *Eur. Phys. J.* **202**, 1 (2012).
- [22] M. E. Cates and J. Tailleur, *Annu. Rev. Condens. Matter Phys.* **6**, 219 (2015).
- [23] J. Elgeti, R. G. Winkler, and G. Gompper, *Rep. Prog. Phys.* **78**, 056601 (2015).
- [24] A. Zöttl and H. Stark, *J. Phys. Cond. Matter* **28**, 253001 (2016).
- [25] B. Liebchen, D. Marenduzzo, and M. E. Cates, *Phys. Rev. Lett.* **118**, 268001 (2017).
- [26] D. Saintillan and M. J. Shelley, *Phys. Rev. Lett.* **100**, 178103 (2008).
- [27] J. S. Guasto, K. A. Johnson, and J. P. Gollub, *Phys. Rev. Lett.* **105**, 168102 (2010).
- [28] K. Drescher, R. E. Goldstein, N. Michel, M. Polin, and I. Tuval, *Phys. Rev. Lett.* **105**, 168101 (2010).
- [29] S. Heidenreich, J. Dunkel, S. H. L. Klapp, and M. Bär, *Phys. Rev. E (R)* **94**, 020601 (2016).
- [30] U. B. Kaupp and L. Alvarez, *Eur. Phys. J. Spec. Top.* **225**, 2119 (2016).
- [31] R. Jeanneret, M. Contino, and M. Polin, *Eur. Phys. J. Spec. Top.* **225**, 2141 (2016).
- [32] J. Stenhammar, C. Nardini, R. W. Nash, D. Marenduzzo, and A. Morozov, *Phys. Rev. Lett.* **119**, 028005 (2017).
- [33] A. Daddi-Moussa-Ider, M. Lisicki, A. J. Mathijssen, C. Hoell, S. Goh, J. Bławdziewicz, A. M. Menzel, and H. Löwen, *J. Phys. Cond. Matter* **30**, 254004 (2018).
- [34] T. Vissers, A. T. Brown, N. Koumakis, A. Dawson, M. Hermes, J. Schwarz-Linek, A. B. Schofield, J. M. French, V. Koutsos, J. Arlt, et al., *Sci. Adv.* **4**, eaao1170 (2018).
- [35] S. Saha, R. Golestanian, and S. Ramaswamy, *Phys. Rev. E* **89**, 062316 (2014).
- [36] O. Pohl and H. Stark, *Phys. Rev. Lett.* **112**, 238303 (2014).
- [37] M. Meyer, L. Schimansky-Geier, and P. Romanczuk, *Phys. Rev. E* **89**, 022711 (2014).
- [38] B. Liebchen, D. Marenduzzo, I. Pagonabarraga, and M. E. Cates, *Phys. Rev. Lett.* **115**, 258301 (2015).
- [39] R. Soto and R. Golestanian, *Phys. Rev. Lett.* **112**, 068301 (2014).
- [40] S. Gonzalez and R. Soto, *New J. Phys.* **20**, 053014 (2018).
- [41] J. L. Anderson, *Ann. Rev. Fluid Mech.* **21**, 61 (1989).
- [42] F. Morrison Jr, *J. Colloid Interface Sci.* **34**, 210 (1970).
- [43] A. Zöttl and H. Stark, *Phys. Rev. Lett.* **112**, 118101 (2014).
- [44] N. Yoshinaga and T. B. Liverpool, *Phys. Rev. E* **96**, 020603 (2017).
- [45] J. Tailleur and M.E. Cates, *Phys. Rev. Lett.* **100**, 218103 (2008).
- [46] Y. Fily and M. C. Marchetti, *Phys. Rev. Lett.* **108**, 235702 (2012).
- [47] J. Bialké, H. Löwen, and T. Speck, *Europhys. Lett.* **103**, 30008 (2013).
- [48] G. S. Redner, M. F. Hagan, and A. Baskaran, *Phys. Rev. Lett.* **110**, 055701 (2013).

- [49] J. Stenhammar, A. Tiribocchi, R. J. Allen, D. Marenduzzo, and M. E. Cates, *Phys. Rev. Lett.* **111**, 145702 (2013).
- [50] D. Levis, J. Codina, and I. Pagonabarraga, *Soft Matter* **13**, 8113 (2017).
- [51] H.-R. Jiang, N. Yoshinaga, and M. Sano, *Phys. Rev. Lett.* **105**, 268302 (2010).
- [52] T. Bickel, G. Zecua, and A. Würger, *Phys. Rev. E* **89**, 050303 (2014).
- [53] V. Prymidis, H. Sielcken, and L. Filion, *Soft Matter* **11**, 4158 (2015).
- [54] M. Rein and T. Speck, *Eur. Phys. J. E* **39**, 84 (2016).
- [55] T. Bäuerle, A. Fischer, T. Speck, and C. Bechinger, *Nat. Comm.* **9**, 3232 (2018).
- [56] L. Wang, M. N. Popescu, F. L. Stavale, A. Ali, T. Gemming, and J. Simmchen, *Soft Matter* (2018).
- [57] A.-P. Hynninen and M. Dijkstra, *J. Phys. Cond. Matter* **15**, S3557 (2003).
- [58] M. Heinen, A. J. Banchio, and G. Nägele, *J. Chem. Phys.* **135**, 154504 (2011).
- [59] E. Schöll-Paschinger, N. E. Valadez-Pérez, A. L. Benavides, and R. Castañeda-Priego, *J. Chem. Phys.* **139**, 184902 (2013).
- [60] J.-X. Sun, *Phys. Rev. B* **75**, 035424 (2007).